Spectrochimica Acta Part A: Molecular and Biomolecular Spectroscopy 105 (2013) 80–87

Contents lists available at SciVerse ScienceDirect

Spectrochimica Acta Part A: Molecular and Biomolecular Spectroscopy

journal homepage: www.elsevier.com/locate/saa

Determination of structural, spectrometric and nonlinear optical features of 2-(4-hydroxyphenylazo)benzoic acid by experimental techniques and quantum chemical calculations

Mehmet Cinar [a,*], Nihat Yildiz [b], Mehmet Karabacak [c], Mustafa Kurt [d]

[a] Department of Science Education, Bayburt University, 69000 Bayburt, Turkey
[b] Department of Physics, Cumhuriyet University, 58140 Sivas, Turkey
[c] Department of Physics, Afyon Kocatepe University, 03040 Afyonkarahisar, Turkey
[d] Department of Physics, Ahi Evran University, 40100 Kirsehir, Turkey

HIGHLIGHTS

- Ground state molecular structure of HABA molecule was optimized.
- Vibrational spectra were examined via FT-IR and FT-Raman techniques and DFT method.
- Electronic transitions were investigated in different solvents.
- Chemical shift were determined depending on predicted and recorded NMR spectra.
- NLO properties were studied theoretically.

GRAPHICAL ABSTRACT

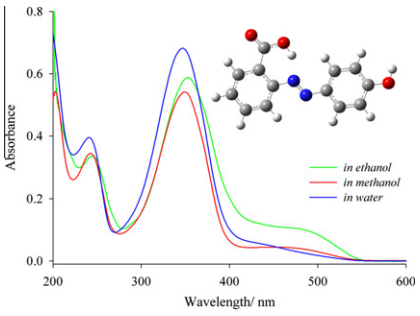

ARTICLE INFO

Article history:
Received 15 October 2012
Received in revised form 1 December 2012
Accepted 6 December 2012
Available online 27 December 2012

Keywords:
2-(4-Hydroxyphenylazo)benzoic acid
Spectroscopic characterization
Quantum chemical calculations

ABSTRACT

The optimized geometrical structure, vibrational and electronic transitions, chemical shifts and nonlinear optical properties of 2-(4-hydroxyphenylazo)benzoic acid (HABA) compound were presented in this study. The ground state geometrical structure and vibrational wavenumbers were carried out by using density functional (DFT/B3LYP) method with 6-311++G(d,p) basis set. The vibrational spectra of title compound were recorded in solid state with FT-IR and FT-Raman spectrometry in the range of 4000–400 cm^{-1} and 4000–10 cm^{-1}; respectively. The fundamental assignments were done on the basis of the recorded spectra and total energy distribution (TED) of the vibrational modes. The ^{1}H and ^{13}C NMR spectra were recorded in deuterated DMSO solution, and gauge–invariant atomic orbitals (GIAOs) method was used to predict the isotropic chemical shifts. The UV–Vis absorption spectra of the compound were observed in the range of 200–800 nm in ethanol, methanol and water solvents. To investigate the nonlinear optical properties, the polarizability, anisotropy of polarizability and molecular first hyperpolarizability were computed. A detailed description of spectroscopic behaviors of compound was given based on the comparison of experimental measurements and theoretical computations.

© 2012 Elsevier B.V. All rights reserved.

Introduction

2-(4-Hydroxyphenylazo)benzoic acid (HABA) can be readily used to determine the amount and biotinbinding activity of avidin in solution, thus, has become important in avidin–biotin technology [1–3]. The binding of HABA to avidin and bovine serum albumin and changes that occur upon protonation are well characterized. Terada et al. [4] recorded the resonance Raman spectra of HABA in aqueous solutions with varying pH, and investigated the effects of the addition of bovine serum albumin and cetyltrimethylammonium bromide. This study shows that

* Corresponding author. Tel.: +90 272 2281311; fax: +90 272 2281235.
E-mail address: mcinar@aku.edu.tr (M. Cinar).

1386-1425/$ - see front matter © 2012 Elsevier B.V. All rights reserved.
http://dx.doi.org/10.1016/j.saa.2012.12.009

the resonance Raman spectrum of HABA in aqueous solution depends critically on the pH. However, in addition, tautomeric equilibrium between azo and hydrazone forms of this molecule must be considered. Hence, Merlin and Thomas [5] studied the resonance Raman spectra of HABA and some deuterated and substituted analogs at neutral, alkaline and acid pH to identify the characteristic bands for each benzenoid ring, to detect the presence of hydrazone and azo forms, and to demonstrate intramolecular coupling effects in the HABA molecule.

Depending on these studies, in the present work, the azo form of monomeric structure of HABA compound was taken into account. A combined experimental and theoretical study was carried out and a detailed description of structural and spectroscopic features of HABA was reported. The ground state molecular structure was optimized and compared with experimental data obtained by X-ray analysis. The FT-IR and FT-Raman spectra were measured in the condensed state. The fundamental vibrational wavenumbers as well as their intensities were predicted by DFT calculations. The complete assignments were performed on the basis of the recorded spectra and total energy distribution (TED) of the vibrational modes. The electronic transitions and isotropic chemical shifts were analyzed via UV–Vis and NMR spectroscopic techniques. All spectroscopic properties which examined by experimental techniques were supported by the computed results. In addition, various nonlinear optical properties such as electric dipole moment, polarizability, anisotropy of polarizability and hyperpolarizability were also addressed theoretically.

Experimental details

The HABA sample was purchased from Sigma–Aldrich company. All commercially available solvents and chemicals were of analytical grade and used without further purification. The FT-IR spectrum of compound was recorded in the region 650–4000 cm^{-1} on a Perkin Elmer FT-IR System Spectrum BX spectrometer calibrated using polystyrene bands. The sample was prepared using a KBr disk technique because of solid state. The spectrum was recorded with a scanning speed of 10 cm^{-1} min^{-1} and the spectral resolution of 4.0 cm^{-1}. FT-Raman spectrum was recorded using 1064 nm line of Nd: YAG laser as excitation wave length in the region 0–3500 cm^{-1} on a Bruker RFS 100/S FT-Raman. The detector is a liquid nitrogen cooled Ge detector. Five hundred scans were accumulated at 4 cm^{-1} resolution using a laser power of 100 mW. The ^{1}H and ^{13}C NMR spectra were recorded in deuterated DMSO ($DMSO_{-d6}$) solution on a Bruker Ultrashield 400 Plus 400 MHz spectrometer using tetramethylsilane (TMS) as an internal reference at 25 °C. The UV absorption spectra were recorded in ethanol, methanol and water solution on Shimadzu UV-1800 PC spectrophotometer in the spectral region of 200–800 nm.

Quantum chemical calculations

The first task for the computational work was to determine the optimized geometry of the compound. The spatial coordinate positions of HABA, as obtained from X-ray structural analysis, were used as the initial coordinates for the theoretical calculations [6]. DFT computations were performed by using the closed-shell Becke–Lee–Yang–Parr hybrid exchange–correlation three-parameter functional (B3LYP) in combination with 6-311++G(d,p) basis set to derive the complete geometry optimization and normal-mode analysis on isolated entities [7–9]. In order to correct the overestimations arising from some negative factors such as basis set truncation effect, neglecting electron correlations and anharmonicity characters of the vibrational modes, the calculated wavenumbers were scaled using two different scaling factors, i.e., 0.983 up to 1700 cm^{-1} and 0.958 for greater than 1700 cm^{-1} [10,11] and thus were fitted to the corresponding experimental wavenumbers. Total energy distribution (TED) calculations were carried out by scaled quantum mechanical (SQM) method [12] using the output files created at the end of the frequency calculations. The Raman scattering activities (S_{Ra}) calculated in the harmonic frequency calculations were converted to relative Raman intensities (I_{Ra}) using the relationship derived from the intensity theory of Raman scattering [13,14].

The simulated IR and Raman spectra were plotted using pure Lorentzian band shapes with full width at half maximum (FWHM) of 10 cm^{-1}. The optimized geometries were used to compute the lowest six singlet → singlet spin-allowed electronic vertical excitation energies at the time dependent-DFT (TD-DFT) level employing B3LYP functional with standard Pople basis set that includes diffuse functions on all atoms (6-311++G(d,p) and 6-311++G(df,pd)). The configuration interaction singles (CISs) [15] technique was also applied with 6-31G(d), 6-311++G(d,p) and 6-311++G(df,pd) basis sets to investigate the excited state calculations. The electronic properties, such as frontier molecular energies, dipole moments, absorption wavelengths and oscillator strengths were calculated. Beside the investigation of isolated molecule, solvent effects were also taken into account. Calculations on proton and carbon magnetic shielding values were carried out using the gauge–invariant atomic orbital (GIAO) approach [16,17] for gas phase and solvent phase. This approach allows the computation of the absolute chemical shielding due to the electronic environment of the individual nuclei. The chemical shift values were determined theoretically by applying the same level of theory on an isolated molecule of tetramethylsilane (TMS). DFT has also been used to calculate the dipole moment, mean polarizability and first static hyperpolarizability based on the finite field approach. The vibrational modes were assigned on the basis of TED analysis using PQS program [18]. The structural and spectroscopic characterization of steady molecule was carried out using Gaussian 09 program package on the personal computer [19].

Results and discussion

Ground state structural properties

The optimized molecular geometry of the monomeric structure of HABA is shown in Fig. 1. The complete optimized geometrical parameters are given in Table 1 in accordance with the atom numbering scheme given in Fig. 1. The available experimental data [6] obtained by the X-ray analysis of HABA compound were also given in Table 1 for comparison. As discussed by Johnson et al. [20], DFT method predicts bond lengths which are systematically too long. From Table 1 one can find that all optimized C—C bond lengths are larger than the experimental values, due to the theoretical

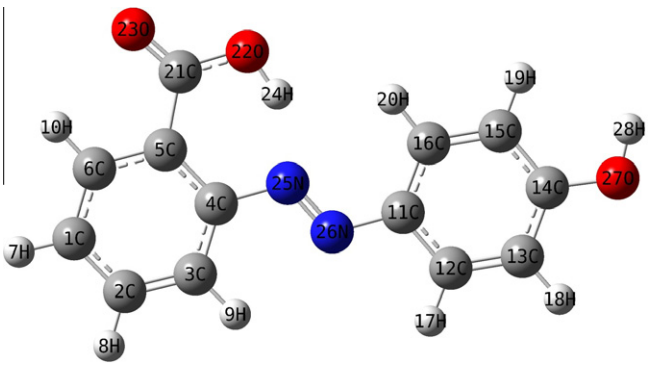

Fig. 1. Optimized geometric structure for ground state with atoms numbering.

calculations belong to isolated molecule in gas phase and the experimental results belong to molecule in solid state. While the optimized C—C bonds of the rings lie in the range of 1.383–1.415 Å, the experimental values observed in the range of 1.370–1.413 Å. Similarly the bond of C—COOH was predicted 0.023 Å larger than recorded one. Similar effect was found for C—O bonds, except C21—O23. However, the C—N and N=N bonds were computed shorter than the experimental results. It is known that the X-ray diffraction method does not inform properly about hydrogen bonds. One should apply the neutron diffraction method which informs on the position of nuclei and not on the electron density distribution. In the reference study [6], hydrogen atoms were inserted in the calculated positions, assigned by the fixed isotropic thermal parameters at the equivalent isotropic *U* of the atoms to which they are attached. Therefore, in this study, the hydrogen bonds and angles of monomeric structure were not discussed in the light of reported data. According to DFT calculations all atoms of HABA form a planer molecule, as also supported by reported X-ray analysis result [6] with the torsion angle of 178.9° (C—N=N—C). The computed bond angles show an excellent agreement with recorded values. The mean deviation was observed as 0.8°. The predicted intramolecular hydrogen bonding of N25···H24 at 2.571 Å is found just 0.01 Å larger than the experimental one.

From the analysis of the two datasets (calculated vs experimental, see Table 1) it can be concluded that the calculated geometry for the monomer in vacuum is in good agreement with the X-ray data, indicating that, in the condensed phase, the intermolecular interactions introduce only relatively unimportant effects on the electron distribution in HABA molecule.

Vibrational analysis

The recorded (FT-IR and FT-Raman) and calculated vibrational wavenumbers along with their relative intensities and tentative assignments with TED of title molecule are given in Table S1 (Supplementary materials). Previously reported resonance Raman spectral data in neutral and alkaline solution of investigated compound are also presented in Table S1 for comparison with our results. The theoretical spectra were obtained from the B3LYP/6-311++G(d,p) method using Lorentzian band shape with band width on half-height 10 cm^{-1}. This reveals good correspondence between theory and experiment in main spectral features. The computed vibrational wavenumbers and the atomic displacements corresponding to the different normal modes were used for identifying the vibrational modes unambiguously. For a visual comparison, the experimental and theoretical spectra are presented in Fig. 2 and Fig. S2, respectively.

Table 1
The optimized geometrical parameters of HABA (predicted by B3LYP/6-311++G(d,p)) and comparison with experimentally identified crystallographic structure, bond lengths in angstrom (Å) and angles in degrees (°).

Bond lengths	Exp.[a]	B3LYP	Bond angles	Exp.[a]	B3LYP
C1—C2	1.388	1.398	C2—C1—C6	120.0	119.9
C1—C6	1.377	1.388	C1—C2—C3	120.4	120.1
C2—C3	1.370	1.385	C2—C3—C4	119.7	120.3
C3—C4	1.391	1.403	C3—C4—C5	120.5	120.0
C4—C5	1.400	1.415	C3—C4—N25	123.0	122.4
C4—N25	1.425	1.419	C5—C4—N25	116.5	117.5
C5—C6	1.386	1.399	C4—C5—C6	118.7	118.5
C5—C21	1.496	1.519	C4—C5—C21	124.9	125.8
C11—C12	1.388	1.405	C6—C5—C21	116.4	115.7
C11—C16	1.393	1.407	C1—C6—C5	120.7	121.2
C11—N26	1.411	1.403	C12—C11—C16	119.6	119.1
C12—C13	1.371	1.385	C12—C11—N26	115.2	115.2
C13—C14	1.381	1.397	C16—C11—N26	125.2	125.8
C14—C15	1.393	1.404	C11—C12—C13	120.2	121.1
C14—O27	1.349	1.358	C12—C13—C14	120.0	119.4
C15—C16	1.370	1.383	C13—C14—C15	120.3	120.2
C21—O22	1.323	1.339	C13—C14—O27	117.8	117.4
C21—O23	1.209	1.207	C15—C14—O27	121.8	122.4
N25—N26	1.266	1.256	C14—C15—C16	119.6	120.2
O22—H24	0.820	0.990	C11—C16—C15	120.2	120.1
O27—H28	0.820	0.964	C5—C21—O22	118.2	117.5
C—$H_{average}$	0.93	1.083	C5—C21—O23	122.4	121.2
N25···H20	2.561	2.571	O22—C21—O23	119.4	121.3
			C21—O22—H24	109.5	108.3
			C4—N25—N26	115.7	116.6
			C11—N26—N25	115.2	117.1
			C14—O27—H28	109.5	110.4

[a] Taken from Ref. [6].

The existence of one or more aromatic rings in a structure is normally readily determined from the C—H and CCC ring related vibrations. The bands due to the ring C—H stretching vibrations are observed as a group of partially overlapping absorptions in the region 3100–3000 cm^{-1}. HABA compound has eight C—H moiety and therefore, eight C—H stretching modes are expected. In FT-IR spectrum two bands located at 3036 and 3097 cm^{-1} were assigned due to C—H stretching. The corresponding calculated wavenumbers were obtained from 3025 to 3080 cm^{-1}. As indicated by TED, these modes involve exact contribution of >95% suggesting that they are pure stretching modes. Vibrations resulting due to C—H in-plane bending appear in the region 1300–1000 cm^{-1} and generally mixed with C—C stretchings. In this study, C—H in-plane bending modes were assigned in 1111–1278 cm^{-1} region in FT-IR spectrum. Two Raman bands were also recorded in this region. The bands computed at 1161, 1189, 1273 and 1309 cm^{-1} are found missing with experimental values. However, they matched with resonance Raman spectral data with quite high accuracy [5]. Skeletal vibrations, involving C—C stretching within the ring, absorb in the 1600–1585 cm^{-1} and 1500–1400 cm^{-1} regions [21]. Varsanyi [22] observed five bands at 1625–1590, 1590–1575, 1540–1470, 1430–1465 and 1380–1280 cm^{-1} for carbon–carbon stretching vibrations of benzene derivatives. In the present study, the pure or dominated vibrations due to C—C stretching were obtained in the region 1325–1620 cm^{-1}. In lower frequency region also some C—C stretching modes mixed with other vibrational modes and with small amount contributions were assigned based on TED results. The C—H out-of-plane bending modes are observed in the region 1000–750 cm^{-1} where the most prominent and informative bands in the spectra of aromatic compounds occur. From TED results, the most of these modes were assigned as pure vibrations.

CCC in-plane and CCCC out-of-plane bendings are the modes associated with smaller force constants than the stretching ones, and hence assigned to lower frequencies. The in-plane ring deformation modes are recorded at higher spectral region than out-of-plane vibrations. However, our assignments show that some in-plane bendings of HABA compound are occur lower region than out-of-plane vibrations (see Table S1). The modes 23, 24, 42 and 44 were assigned to ring deformation for monomeric HABA molecule basing on TED results.

The vibrational analysis of carboxylic acid (COOH) group is made on the basis of carbonyl group and hydroxyl group vibrations. The O—H stretching vibration is characterized by a very strong peak in Raman as compared to the corresponding peak in infrared regions. The O—H group stretching vibrations are likely to be most sensitive to the environment, so they show pronounced shifts in the spectra of the hydrogen bonded species. A free hydroxyl group or a non-hydrogen bonded hydroxyl group absorbs in the range 3700–3500 cm^{-1}. In the case of the un-substituted phenols, the frequency of O—H stretching vibration was observed at 3657 cm^{-1} in the gas phase [23]. In our case, the predicted band at 3665 cm^{-1} missing with recorded data was assigned to hydroxyl group vibration. The O—H stretching vibration of carboxyl group was recorded at 3163 cm^{-1} in FT-IR and calculated at 3120 cm^{-1}.

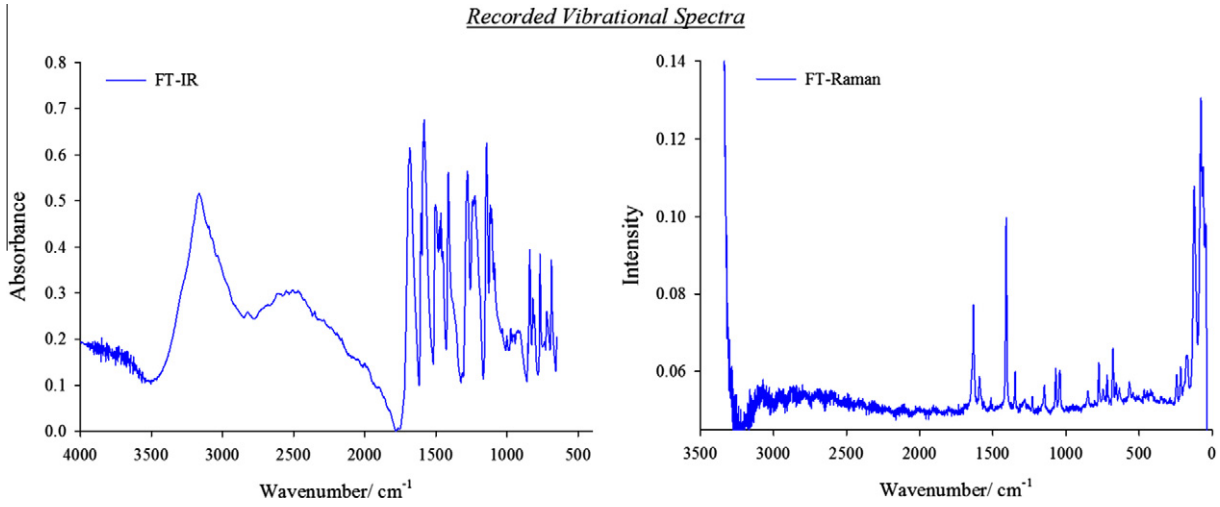

Fig. 2. Experimental (FT-IR and FT-Raman, in solid phase) vibrational spectra.

The C—O stretching band of the aromatic compounds in IR spectrum is characterized by the frequencies around 1270–1230 cm^{-1}, while the band in Raman spectrum usually presents a weak activity in the region of 1210–1310 cm^{-1}. However, it is known that C—O stretching and O—H bending modes are not independent vibrational modes because they coupled with the vibrations of adjacent groups. Therefore, we are not dealing with C—O stretching vibration, but with coupled asymmetric vibration involving C—C—O stretching. The band obtained with FT-IR/FT-Raman at 1226/1229 cm^{-1} and the band calculated at 1273 cm^{-1} missing with experimental data was assigned to C—C—O stretching with contribution of 33% and 15%, respectively. The ring-hydroxyl group stretching observed in FT-IR at 1278 cm^{-1} contributed with 50%. The O—H in-plane bending vibrations occur in the general region of 1420–1330 cm^{-1} and are not much affected due to hydrogen bonding unlike the stretching and out-of-plane bending frequencies. The FT-IR bands observed at 1475 and 1504 cm^{-1} (modes 61 and 62) were assigned to O—H bending vibration of carboxylic group, and found out of the general region given above which may cause due to helical packing form of HABA compound [6]. The in-plane banding mode of hydroxyl group was recorded at 1349 cm^{-1} in FT-Raman spectrum and computed at 1351 cm^{-1} with 20% contribution. The band calculated at 1172 with 53% contribution was also assigned to in-plane bending mode of hydroxyl group. The bands appearing in FT-IR/FT-Raman at 819/776 cm^{-1}, respectively, were assigned to out-of-plane O—H bending vibration of carboxylic group, and corresponding mode of hydroxyl group was calculated at 350 cm^{-1}.

The appearance of strong bands in the FT-IR and weak bands in the Raman spectra (less polarizability resulting due to highly dipolar carbonyl bond) around 1800–1650 cm^{-1} in aromatic compounds is the most salient feature of the presence of carbonyl group and are due to the C=O stretching motions. The wavenumber of the C=O stretch due to carbonyl group mainly depends on the bond strength, which in turn depends upon inductive, conjugative, steric effects and the lone pair of electrons on oxygen. The band appearing at 1683 cm^{-1} as a very strong band in FT-IR was assigned to C=O stretching vibration. The corresponding predicted mode was found at 1722 cm^{-1}. As indicated by TED, this mode involves exact contribution of 80% suggesting that it is a pure stretching mode.

The N=N stretching is the characteristic vibrational mode of the azo compounds. This mode was obtained at 1443 cm^{-1} (Raman) and 1511 cm^{-1} (IR) for trans and cis forms of azobenzene, respectively [24,25]. Merlin and Thomas [5] observed a strong band at 1410 cm^{-1} characteristic of the azo form of HABA in nonenhanced Raman spectra obtained with the 647.1 nm line. On the other hand, in resonance Raman spectra obtained with the 514.5 nm lines, a weak band around 1400 cm^{-1} and a strong line in the 1600 cm^{-1} region was obtained which suggests the hydrazone form of HABA. In this study, N=N stretching mode of HABA compound recorded at 1413 cm^{-1} in FT-IR and 1408 cm^{-1} in FT-Raman spectrum. The corresponding resonance Raman band in neutral and alkaline solution were observed at 1416 and 1407 cm^{-1}, respectively [5]. In addition, our TED calculations show that the FT-Raman band at 1511 cm^{-1} (calculated at 1520 cm^{-1}) is also arising from N=N stretching.

Assigning the C—N stretching wavenumber is a rather difficult task since there are problems in identifying these wavenumbers from other vibrations. Silverstein et al. [26] assigned the C—N stretching absorption in the region 1382–1266 cm^{-1} for aromatic amines. In numerous azo compounds the band at 1140 cm^{-1} is attributed to C—N stretching. We observed this band at 1144 cm^{-1} in FT-IR and 1148 cm^{-1} in FT-Raman. The Raman active C—N symmetric band was assigned at 1143 cm^{-1} for trans-azobenzene [27–29]. The FT-IR band at 1119 cm^{-1} contributes the C—N stretching. While the FT-IR band at 1241 cm^{-1} arises from the asymmetric phenyl ring-N stretching, the calculated band at 1189 cm^{-1} and supported by previously reported resonance Raman band (1189 cm^{-1}) is due to symmetric stretching of this mode [5].

NMR chemical shifts

Due to their sensitivity to conformational variations, chemical shifts (c.s.) are valuable for structural interpretation and recognized as an imperative part of the information contained in NMR spectra. It is well-known that the combined use of NMR spectroscopic technique and computer simulation methods offers a powerful way to interpret and predict the even structure of large biomolecules [30]. Thus, we followed same methodology to identify the magnetic properties of steady compound. The experimentally observed ^{1}H and ^{13}C NMR spectra of HABA compound (with respect to TMS, and in $DMSO_{-d6}$ solution) are shown in Fig. 3. Theoretically isotropic chemical shifts were also calculated with respect to TMS, and therefore, as first task the c.s. of TMS were calculated using the same method. Theoretical and experimental c.s. of HABA in ^{1}H and ^{13}C NMR spectrum are gathered in Table S2. The reference values of TMS are also given in the bottom of Table S2.

The chemical shifts of aromatic protons of organic molecules are usually observed in the range of 7.00–8.00 ppm. In this study, the eight protons attached to the rings resonance in the range of 6.97–7.79 ppm, as expected. The theoretical results obtained using two basis sets show a quite good agreement with the experimental data. For the aromatic protons the chemical shift of the H10 was predicted in the lowest field, and the most deviation from measured results was also obtained for this atom. This pattern may rise due to the attraction of H10 and O23. The protons on the oxygen atoms were recorded at 13.06 and 10.40 ppm. It is known that the carboxylic acids exist as a stable hydrogen-bonded dimers in nonpolar solvents, therefore carboxylic proton absorbs in a characteristic range 13.2–10.0 ppm. The intramolecular O22—H24···N25 type hydrogen bond between the carboxylic group oxygen atom and nitrogen atom forming a six member ring to reduce the energy of HABA [6]. Therefore, the signal recorded at 13.06 ppm was assigned to COOH resonance. The phenolic proton peak is usually a sharp singlet and observed in the range 4.0–7.5 ppm depending on concentration, solvent and temperature. In the present study, the chemical shift of phenolic oxygen was predicted in the range 4.19–5.20 ppm (see Table S2). However, Qian and Hang [6] reported that the HABA compound form in an infinite hellical structure, and the presence of the solvent water molecules play a key role in this packing. The O—H···O intermolecular hydrogen bonds between the phenolic oxygen atom of HABA and solvent water molecule forming this structure, and leads to a more significant downfield shift of the isotropic chemical shifts. The observed signal at 10.40 ppm is an evidence for existing of interaction between solute–solvent molecules. To predict the chemical shift of proton on oxygen atoms, calculations were done for neutral molecule containing hydrogen bonds with water molecules (see Fig. S1) and results are presented in Table S3. The chemical shift of hydroxyl proton was calculated at 15.0–16.0 ppm in the view of the hydrogen bonding, and this considerable deviation shows that the interaction between solvent water molecule and OH group changes the electronic environment of H28 proton significantly.

Generally, aromatic carbon resonances occur between 100–150 ppm. However, on the attachment of more than one electron-withdrawing and electron-releasing substituents, this shift range may expand to 90–180 ppm. On the other hand, the carbonyl carbons (C=O) have a low-lying excited state involving the movement of electrons from the oxygen lone pair to antibonding π orbital that generates a paramagnetic current. This $n \rightarrow \pi^*$ transition causes the large shift to high frequency, thus, the carbonyl carbon signals have a smaller intensity and appear in a characteristic field, 150–220 ppm [31], makes it easier to recognize the carbonyl absorptions from the other resonances. In this study, low-field shift of carbonyl carbon (C21) was recorded in ^{13}C NMR spectrum at 168.5 ppm in $DMSO_{-d6}$ solution. The signal of other carbon atom that OH group is attached (C14) was also observed in this field (161.3 ppm). This signal was observed at 159.2 ppm for para-OH substituted dimethylaminoazobenzene in $CDCl_3$ [32], and 160.2 ppm for 1-(2′-chloro-4′-nitrophenylazo)-2,4-benzenediol in DMSO solution [33]. Because of the electronegative feature of the nitrogen atom, the phenyl-azo group carbon atoms (C4 and C11) resonance at lower field, and the signal of these carbon atoms were recorded at 150.7 and 145.4 ppm. Same tendency was observed for some disperse azobenzene dye molecules [34]. A quick look at the Table S2 and Fig. 3 shows that the recorded c.s. of the aromatic carbons lie in the range 115.9–131.5 ppm, and computed results are described fairly well by the selected method combined with the basis sets.

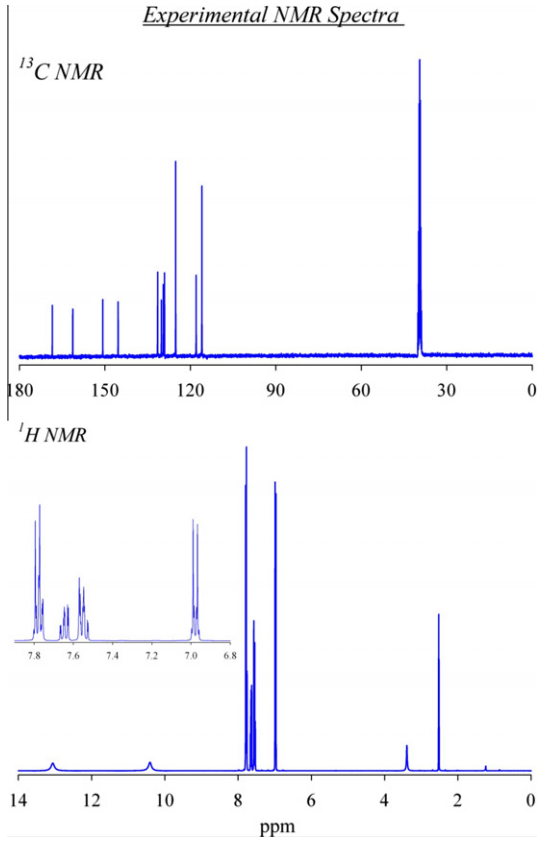

Fig. 3. Experimental ^{1}H and ^{13}C NMR spectra (with respect to TMS and in DMSO solution).

UV–Vis studies and electronic properties

The electronic absorption spectra of HABA compound were recorded in ethanol, methanol and water solution, shown in Fig. 4. On the basis of a fully optimized ground state structure, both TD-DFT and CIS were used to determine the low-lying excited states of HABA. The 6-311++G(d,p) and 6-311++G(df,pd) basis sets were applied for both methods, additionally 6 311G(d) set was used for CIS calculations. The simulated UV–Vis spectra of studied molecule were given in Fig. S3a–e (Supplementary materials). The experimental peaks together with the absorbance values and excitation energies are presented in Table 2. The TD-B3LYP computed electronic vertical singlet transition energies, oscillator strength (*f*), absorption wavelength (λ) and transition levels of HABA molecule for gas phase and all solvents are shown in Table S4 (Supplementary materials) whereas the same calculations obtained by CIS method are presented in Table S5 (Supplementary materials).

Due to the conjugation between azobenzene and the aromatic ring system, aromatic azo compounds generally exhibit a low intensity n–π^* absorption band in the visible range and a high intensity π–π^* band in the UV range [35,36]. The absorption spectrum of HABA compound gave a maximum π–π^* absorption at 358.5 nm [6]. In earlier studies, this major band from the visible absorption spectrum of free dye in neutral medium was observed at 348 nm [1,37]. It was seen that the binding of HABA by serum albumin shifts this absorption band of the dye to shorter wavelength, from 370 to 410 nm depending on the type of the albumin used [37]. In addition, binding by albumin causes an appearance of new band at 480 nm [37]. The visible absorption at 480 nm obtained from the resonance a Raman spectrum of HABA was also marked as an evidence of participation of the azo-hydrazone tautomerism [4]. A similar band was observed for solutions of HABA in organic solvents such as ethanol dimethylsulphoxide or dimethylformamide [37]. The π–π^* and n–π^* transitions for 4-

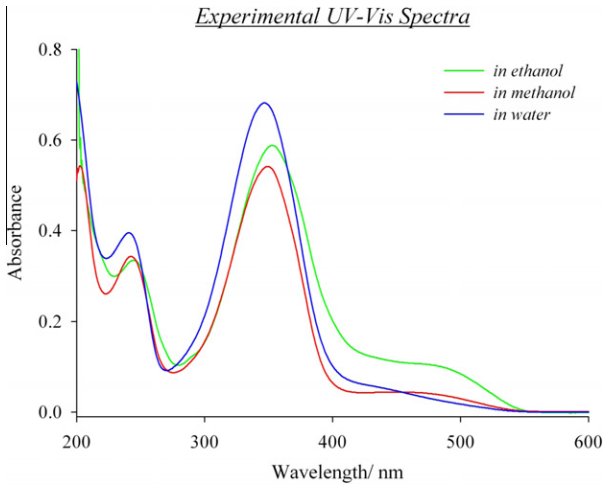

Fig. 4. Experimental UV–Vis spectra.

Table 2
Experimentally obtained absorption wavelength λ (nm), excitation energies E(eV) and absorbance values of HABA.

Ethanol			Methanol			Water		
E(eV)	λ (nm)	Abs.	E(eV)	λ (nm)	Abs.	E(eV)	λ (nm)	Abs.
2.6042	480.0	0.103	2.7778	450.0	0.044			
3.5411	353.0	0.588	3.5714	350.0	0.541	3.5971	347.5	0.682
5.1125	244.5	0.335	5.1546	242.5	0.344	5.1975	240.5	0.395

((4-hydroxyphenyl)azo)benzoic acid were recorded at 356 and 431 nm, respectively, in methanol [38]. We recorded the major band of HABA compound at 353.0, 350.0 and 347.5 nm for ethanol, methanol and water solution, respectively. The observed maximum absorption peak for all solutions was assigned as π–π^* transition. The TD-DFT method predicted the maximum absorption peak at near 396 nm with strong oscillator strength of solvated molecule, and this electronic absorption corresponds to the transition from the ground to the first excited state and is mainly described by one electron excitation from the highest occupied molecular orbital (HOMO) to the lowest unoccupied molecular orbital (LUMO). It is seen that the TD-B3LYP method overestimates the major absorption band. On the contrary, CIS method underestimated this electronic excitation, and predicted at near 310 nm using with the largest basis sets.

It is known that, the UV–Vis absorption spectra of trans-azobenzenes is characterized by a band in region 440–480 nm originates from symmetry-forbidden n–π^* transitions occurring at the central nitrogen atoms [39]. As expected, a broad band at 480.0 nm was observed in ethanol solution whereas this band shifted to 450.0 nm for methanol. No absorption was recorded in this region when the compound dissolved in water. This excitation is concerned with the HOMO-1 (orbital 62) → LUMO electronic transitions which corresponds to n–π^* transition (see Fig. S3) and well predicted by TD-B3LYP method. The third band recorded at 244.5, 242.5 and 240.5 nm in ethanol, methanol and water, respectively, is localized on the phenyl groups and originates from π–π^* transition. This band was observed at 241 nm in previous study [40].

The most important orbitals in a molecule are the frontier molecular orbitals. These orbitals determine the way the molecule interacts with other species. The energy values of frontier molecular orbitals and energy differences between the excitation levels along with the total and components of ground state dipole moment calculated by TD-B3LYP and CIS method are presented in Tables S6 and S7 (Supplementary materials). The atomic orbital compositions of the frontier molecular orbital are sketched in Fig. S4. The dipole moment in a molecule is another important electronic property that results from nonuniform distribution of charges on the various atoms in a molecule. It is mainly used to study the intermolecular interactions involving the van der Waals type dipole–dipole forces, etc., because the larger the dipole moment, stronger will be the intermolecular interactions [41]. Based on predicted dipole moment values (by TD-B3LYP), we can say that in going to the solvent phase from the gas phase, the dipole moment value increases. The dipole moment in solvent phase also increases with increasing of polarity of the solvent. It should be noted that the dipole moment values calculated by TD-DFT method are larger with a small amount than the calculated by CIS method. This trend was obtained for basis sets; larger basis set gives larger values.

NLO properties

Nonlinear optical (NLO) materials have been the subject of intense research, due to their possible application in a wide range of technologies, such as data storage, optical computing and optical communication [42–44]. Therefore, it is known that there has been an intense investigation for molecules with large non-zero hyperpolarizabilities, since these substances have potential as the constituents of non-linear optical materials. The azo containing systems have a special significance among the many molecular designs that are used for introducing NLO behavior [45,46]. Due to their peculiar photoswitching properties, azobenzenes are used in many areas of molecular electronics and suitable for various kinds of applications [47–49].

An organic donor-π–acceptor (electro donor (OH)–acceptor unit (COOH)) compound HABA has an asymmetric charge distribution and acentric crystal packing. Thus, it may be a good candidate for NLO materials. In present study, the electronic dipole moment, molecular polarizability (α_{tot}), anisotropy of polarizability ($\Delta\alpha$) and molecular first hyperpolarizabiliy (β_{tot}) of present compound were investigated, and results are gathered in Table 3. The mathematical details used for the calculations were reported in our earlier publications [50,51]. The dipole moment obtained by the frequency job output file is equal to 5.7050 D for gas phase. The highest value of dipole moment is observed for component μ_x. In this direction, this value is equal to 4.3315 D whereas the component μ_z is nearly equal to zero. Total polarizability calculated as 32.420×10^{-24} esu. The first hyperpolarizability value of the title compound is equal to 21.06×10^{-30} esu. The theoretical calculation of β components is very useful as this clearly indicates the direction of charge delocalization. Domination of particular component indicates on a substantial delocalization of charges in this direction. Therefore, the largest β_{xxx} value indicates charge delocalization is perpendicular to the bond axis and the involvement of π orbitals in intra-molecular charge transfer process.

As we know, the NLO properties of HABA have not been measured by experimental techniques till now. On the other hand, Smitha et.al [38] reported the synthesis of a series of new AB type azobenzene monomers including 4-((4-hydroxyphenyl)azo)benzoic acid (the COOH group at para position according to HABA) and the measurement of their hyperpolarizability tensor β in methanol by the HRS technique. The ground state dipole moment and first hyperpolarizability of mentioned compound was reported as 2.850 D and 17.16×10^{-30} esu [52]. Urea is one of the prototypical molecules used in the study of the NLO properties of molecular systems. Therefore it was used frequently as a threshold value for comparative purposes. Cassidy et al. [53] measured the second and third order hyperpolarizabilities of this molecule using the DC field

Table 3
Calculated NLO properties of free HABA, molecular polarizability (α_{tot}), anisotropy of polarizability ($\Delta\alpha$), molecular first hyperpolarizabiliy (β_{tot}), electronic dipole moment and their components.

	Gas		Methanol			Gas		Methanol	
	a.u.	esu ($\times10^{-24}$)	a.u.	esu ($\times10^{-24}$)		a.u.	esu ($\times10^{-30}$)	a.u.	esu ($\times10^{-30}$)
α_{xx}	376.0093	55.7246	536.1981	79.4646	β_{xxx}	−2457.9371	−21.2349	−8941.4936	−77.2482
α_{xy}	13.7794	2.0421	18.1683	2.6925	β_{xxy}	−394.9466	−3.4121	−1216.6898	−10.5113
α_{yy}	190.8907	28.2900	269.3741	39.9212	β_{xyy}	91.7055	0.7923	121.3840	1.0487
α_{xz}	0.0028	0.0004	0.0041	0.0006	β_{yyy}	46.6339	0.4029	436.5192	3.7712
α_{yz}	0.0019	0.0003	0.0034	0.0005	β_{xxz}	−0.0457	−0.0004	−0.1311	−0.0011
α_{zz}	89.3723	13.2450	120.8710	17.9131	β_{xyz}	0.0064	0.0001	0.0132	0.0001
α_{tot}	218.7575	32.4199	308.8144	45.7663	β_{yyz}	0.0010	0.0000	−0.0322	−0.0003
$\Delta\alpha$	252.8585	37.4736	365.8725	54.2223	β_{xzz}	−37.5277	−0.3242	−89.6269	−0.7743
μ_x	4.3315		5.6544		β_{yzz}	−57.0326	−0.4927	−99.9538	−0.8635
μ_y	−3.7128		−4.6653		β_{zzz}	0.0100	0.0001	−0.0015	0.0000
μ_z	0.0009		0.0012		β_{tot}	2437.6963	21.0600	8953.1013	77.3485
μ_{tot}	5.7050		7.3306						

induced second harmonic generation and four-wave mixing techniques. From these measurements, the β value of urea was reported as 2.3×10^{-30} esu. Hence, our calculations show that the β value of HABA is larger than the magnitude of urea [54]. With respect to our calculations, DFT did not give appropriate and quantitatively accurate results for NLO properties in comparisons with experiment [52,54].

Conclusion

The ground state geometry, vibrational wavenumbers and assignments of vibrational modes, magnetic properties depending on NMR analysis, UV–Vis spectra in various solvents, electronic transitions and nonlinear optical properties of HABA compound were investigated. The ground state geometrical parameters of monomeric structure were predicted by DFT calculations with a quite high accuracy when compared with X-ray analysis of compound. The scaled vibrational frequencies show a quite good agreement with recorded FT-IR and FT-Raman spectral vibrations especially in the region lower 3000 cm^{-1}. All vibrational modes were assigned based on experimental observations together with the results of TED calculations. To clarify the magnetic properties of the title compound, ^1H and ^{13}C NMR spectra were recorded in $DMSO_{-d6}$ solution and compared with theoretically obtained chemical shifts via GIAO method and a fairly large and flexible two basis sets, 6-311++G(d,p) and 6-311++G(df,pd). Because of the hydrogen-bonded association between HABA compound and solvent water molecule, the NMR calculations were examined for isolated molecule and with water molecules. When the interaction between solute and solvent molecules was taken into account, the chemical shift of hydroxyl proton was predicted in the higher range, and there is still considerable deviation from recorded value which means a stronger electronic distribution exists in experimental conditions. Therefore, it can be seen from our results that for the hydrogen bonded molecules intermolecular interactions should be taken into account to predict the magnetic properties. The electronic absorption features of HABA compound were evaluated via experimental and theoretical UV–Vis spectral analysis which were provided insight into the excitation energy and oscillator strength and predicted the major electronic excitation as $\pi \rightarrow \pi^*$ type at about 350 nm in ethanol, methanol and water solution. The observed additional absorption peak for organic solvents in visible range was predicted quite well by TD-B3LYP method. The results of computations of spectroscopic parameters of lowest-lying electronic excited states of HABA support the analysis of experimentally recorded spectra. The NLO properties of studied molecule were investigated by quantum chemical DFT calculations, and since the experimental data are not available, results were compared with urea which is one of the prototypical molecules used in the study of the NLO properties of molecular systems. The first hyperpolarizability value of HABA was found larger than the magnitude of urea, and, therefore, HABA may be a candidate of nonlinear optical materials.

Appendix A. Supplementary material

Supplementary data associated with this article can be found, in the online version, at http://dx.doi.org/10.1016/j.saa.2012.12.009.

References

[1] N.M. Green, Biochem. J. 94 (1965) 23c–24c.
[2] N.M. Green, Methods Enzymol. 18 (1970) 418–424.
[3] M. Wlchek, E.A. Bayer (Eds.), Avidin-Blotm Technology. Methods Enzymol, vol. 184, Academic Press, San Diego, 1990.
[4] H. Terada, B.-K. Kim, Y. Saito, K. Machida, Spectrochim. Acta 31A (1975) 945–949.
[5] J.C. Merlin, E.W. Thomas, Spectrochlm. Acta 35A (1979) 1243–1249.
[6] H. Qian, W. Huang, J. Mol. Struct. 743 (2005) 191–195.
[7] A.D. Becke, J. Chem. Phys. 98 (1993) 5648–5652.
[8] C. Lee, W. Yang, R.G. Parr, Phys. Rev. B 37 (1988) 785–789.
[9] P. Perdew, Y. Wang, Phys. Rev. B 45 (1992) 13244–13249.
[10] M. Karabacak, M. Cinar, Z. Unal, M. Kurt, J. Mol. Struct. 982 (2010) 22–27.
[11] N. Sundaraganesan, S. Ilakiamani, H. Saleem, P.M. Wojciechowski, D. Michalska, Spectrochim. Acta A 61 (2005) 2995–3001.
[12] J. Baker, A.A. Jarzecki, P. Pulay, J. Phys. Chem. A 102 (1998) 1412–1424.
[13] G. Keresztury, S. Holly, J. Varga, G. Besenyei, A.Y. Wang, J.R. Durig, Spectrochim. Acta A 49 (1993) 2007.
[14] G. Keresztury, J.M. Chalmers, P.R. Griffith (Eds.), Raman Spectroscopy: Theory in Handbook of Vibrational Spectroscopy, John Wiley & Sons Ltd., New York, 2002. vol. 1.
[15] J.B. Foresman, M. Head-Gordon, J.A. Pople, M.J. Frisch, J. Phys. Chem. 96 (1992) 135–149.
[16] R. Ditchfield, J. Chem. Phys. 56 (1972) 5688–5691.
[17] K. Wolinski, J.F. Hinton, P. Pulay, J. Am. Chem. Soc. 112 (1990) 8251–8260.
[18] SQM Version 1.0, Scaled Quantum Mechanical Force Field, 2013 Green Acres Road, Fayetteville, Arkansas, 72703.
[19] M.J. Frisch, G.W. Trucks, H.B. Schlegel, G.E. Scuseria, M.A. Robb, J.R. Cheeseman, G. Scalmani, V. Barone, B. Mennucci, G.A. Petersson, H. Nakatsuji, M. Caricato, X. Li, H.P. Hratchian, A.F. Izmaylov, J. Bloino, G. Zheng, J.L. Sonnenberg, M. Hada, M. Ehara, K. Toyota, R. Fukuda, J. Hasegawa, M. Ishida, T. Nakajima, Y. Honda, O. Kitao, H. Nakai, T. Vreven, J.A. Montgomery Jr., J.E. Peralta, F. Ogliaro, M. Bearpark, J.J. Heyd, E. Brothers, K.N. Kudin, V.N. Staroverov, R. Kobayashi, J. Normand, K. Raghavachari, A. Rendell, J.C. Burant, S.S. Iyengar, J. Tomasi, M. Cossi, N. Rega, J.M. Millam, M. Klene, J.E. Knox, J.B. Cross, V. Bakken, C. Adamo, J. Jaramillo, R. Gomperts, R.E. Stratmann, O. Yazyev, A.J. Austin, R. Cammi, C. Pomelli, J.W. Ochterski, R.L. Martin, K. Morokuma, V.G. Zakrzewski, G.A. Voth, P. Salvador, J.J. Dannenberg, S. Dapprich, A.D. Daniels, Ö. Farkas, J.B. Foresman, J.V. Ortiz, J. Cioslowski, D.J. Fox, Gaussian 09, Revision A.1, Gaussian, Inc., Wallingford, CT, 2009.
[20] B.G. Johnson, P.M. Gill, J.A. Pople, J. Chem. Phys. 98 (1993) 5612–5626.
[21] R.M. Silverstein, F.X. Webster, D.J. Kiemle, Spectrometric Identification of Organic Compouns, seventh ed., John Wiley & Sons, 2005.
[22] G. Varsanyi, Assignments of Vibrational Spectra of 700 Benzene Derivatives, Wiley, New York, 1974.
[23] D. Michalska, D.C. Bienko, A.J. Abkovicz-Bienko, Z. Latajka, J. Phys. Chem. 100 (1996) 17786–17790.

[24] B. Kellerer, H.H. Hacker, J. Brandmuller, Ind. J. Pure Appl. Phys. 9 (1971) 903–909.
[25] V.R. Kubler, W. Luttke, S. Weckherlin, Z. Elektrochem. 64 (1960) 650–654.
[26] M. Silverstein, G.C. Basseler, C. Morill, Spectrometric Identification of Organic Compounds, Wiley, New York, 1981.
[27] S. Koide, Y. Udagawa, N. Mikami, K. Kaya, M. Ito, Bull. Chem. Soc. Jpn. 45 (1972) 3542–3543.
[28] I.K. Barker, V. Fawcett, D.A. Long, J. Raman Spectrosc. 18 (1987) 71–75.
[29] A. Biancalana, E. Campani, G. Gorini, G. Masetti, M. Quaglia, J. Raman Spectrosc. 23 (1992) 155–160.
[30] T. Schlick, Molecular Modeling and Simulation: An Interdisciplinary Guide, second ed., Springer, New York, 2010. vol. 21.
[31] J.B. Stothers, P.C. Lauterbur, Can. J. Chem. 42 (1964) 1563–1576.
[32] V. Koleva, T. Dudev, I. Wawer, J. Mol. Struct. 412 (1997) 153–159.
[33] X.-L. You, C.-R. Lu, Z.-L. Huang, D.-C. Zhang, Dyes Pigments 63 (2004) 217–223.
[34] M. Cinar, PhD Thesis, Sakarya University, 2012.
[35] H. Rau, in: J.F. Rabek (Ed.), Photochemistry and Photophysics, vol. 2, CRC Press, Boca Raton, 1990.
[36] G.S. Kumar, Azo Functional Polymers, Techromic Publ., Lancaster, 1992.
[37] J.H. Baxter, Arch. Biochem., Biophys. 108 (1964) 375–383.
[38] P. Smitha, S.K. Asha, C.K.S. Pillai, J. Polym. Sci. Part A: Polym. Chem. 43 (2005) 4455–4468.
[39] F. Hamon, F. Djedaini-Pilard, F. Barbot, C. Len, Tetrahedron 65 (2009) 10105–10123.
[40] A.O. Aluoch, PhD Thesis, State University of New York, 2007.
[41] D.P. Chemica, Scholar Res. Lib. 2 (2010) 48–58.
[42] J. Zyss (Ed.), Molecular nonlinear optics: materials phenomena and devices, Chem. Phys. 243 (1999) (Special issue).
[43] S.P. Karna (Ed.), Electronics and optical materials, J. Phys. Chem. A 104 (2000) (Special issue).
[44] D.R. Kanis, M.A. Ratner, T.J. Marks, Chem. Rev. 94 (1994) 195–242.
[45] S. Xie, A. Natansohn, P. Rochon, Chem. Mater. 5 (1993) 403–411.
[46] D.M. Burland, R.D. Miller, C.A. Walsh, Chem. Rev. 94 (1994) 31–75.
[47] Z.F. Liu, K. Hashimoto, K. Fujishima, Nature 347 (1990) 658–660.
[48] T. Ikeda, O. Tsutsumi, Science 268 (1995) 1873–1875.
[49] S. Kawata, Y. Kawata, Chem. Rev. 100 (2000) 1777–1788.
[50] M. Cinar, A. Coruh, M. Karabacak, Spectrochim. Acta Part A 83 (2011) 561–569.
[51] M. Karabacak, L. Sinha, O. Prasad, Z. Cinar, M. Cinar, Spectrochim. Acta Part A 93 (2012) 33–46.
[52] We calculated the nonlinear optical properties of 4-[(4-hydroxyphenyl)azo] benzoic acid using same method and basis set of calculations of HABA. The dipole moment was predicted as 7.9876/11.3672 D for gas phase/methanol solution whereas the dipole moment was reported as 2.850 D in methanol. The first hyperpolarizability value determined using hyper-Rayleigh scattering method obtained at 17.16×10^{-30} esu. DFT calculations result this value at $68.8305/252.3481 \times 10^{-30}$ esu for gas phase/methanol solution [Experimental values were taken from Ref. [38].
[53] C. Cassidy, J.M. Halbout, W. Donaldson, C.L. Tang, Opt. Commun. 39 (1979) 243–246.
[54] For comparison with experimental study we calculated the nonlinear optical properties of urea applied with method. The dipole moment of urea was predicted at 4.43 D with in consistency of experimentally recorded value of 4.56 D (Ref. [53]). However, first hyperpolarizability of urea was calculated at 0.81×10^{-30} esu, and experimental value is nearly 2.5 times larger than this result. If the computed results taken into account, β of HABA is larger 26 times than the magnitude of urea. However, when we use the experimental β value of urea (2.3×10^{-30} esu), β of HABA will be 9 times larger than urea. It also should be noted that the experimental results of HABA are not available and thus, the relationship between the calculated and observed β values of urea could be valid for HABA.